Published in final edited form as:
Cell. 2009 January 23; 136(2): 322–336. doi:10.1016/j.cell.2008.11.050.

A centrosomal Cdc20-APC pathway controls dendrite morphogenesis in postmitotic neurons

Albert H. Kim[1,4], **Sidharth V. Puram**[1,2], **Parizad M. Bilimoria**[1,3], **Yoshiho Ikeuchi**[1], **Samantha Keough**[1], **Michael Wong**[5], **David Rowitch**[5,6], and **Azad Bonni**[1,2,3,*]

[1] Department of Pathology, Boston, MA 02115

[2] Program in Biological and Biomedical Sciences, Boston, MA 02115

[3] Program in Neuroscience, Harvard Medical School, Boston, MA 02115

[4] Department of Neurosurgery, Brigham and Women's Hospital, Boston, MA 02115

[5] Institute for Regeneration Medicine, Howard Hughes Medical Institute, San Francisco, CA 94143

[6] Departments of Pediatrics and Neurosurgery, UCSF, San Francisco, CA 94143

SUMMARY

The ubiquitin ligase anaphase-promoting complex (APC) recruits the coactivator Cdc20 to drive mitosis in cycling cells. However, the nonmitotic functions of Cdc20-APC have remained unexplored. We report that Cdc20-APC plays an essential role in dendrite morphogenesis in postmitotic neurons. Knockdown of Cdc20 in cerebellar slices and in postnatal rats in vivo profoundly impairs the formation of granule neuron dendrite arbors in the cerebellar cortex. Remarkably, Cdc20 is enriched at the centrosome in neurons, and the centrosomal localization is critical for Cdc20-dependent dendrite development. We also find that the centrosome-associated protein histone deacetylase 6 (HDAC6) promotes the polyubiquitination of Cdc20, stimulates the activity of centrosomal Cdc20-APC, and drives the differentiation of dendrites. These findings define a novel postmitotic function for Cdc20-APC in the morphogenesis of dendrites in the mammalian brain. The identification of a centrosomal Cdc20-APC ubiquitin signaling pathway holds important implications for diverse biological processes including neuronal connectivity and plasticity.

INTRODUCTION

The proper development and patterning of dendrites is essential for the establishment of neuronal connectivity. Dendrites represent the critical receptive limb of neurons, and accordingly the morphology of the dendritic arbor influences the processing of synaptic information within a neural circuit (Parrish et al., 2007). Perturbations in dendrite morphology are thought to play critical roles in the pathogenesis of diverse neurological disorders including Down's, Fragile X, and Rett syndromes as well as adult neurodegenerative diseases (Kaufmann and Moser, 2000; Knobloch and Mansuy, 2008). Therefore, elucidation of the molecular mechanisms governing dendrite differentiation not only deepens our understanding of neuronal circuitry but also potentially provides insight into diseases that affect the human brain.

*Correspondence: E-mail: azad_bonni@hms.harvard.edu.

Neurons are postmitotic cells that exit the cell cycle permanently. However, components of the cell cycle machinery are expressed in neurons (Becker and Bonni, 2005; Greene et al., 2004). In proliferating cells, protein ubiquitination plays an essential role in coordinating the events of the cell cycle. The anaphase-promoting complex (APC) is an evolutionarily conserved, multisubunit ubiquitin ligase that is critical for normal cell cycle transitions (King et al., 1995; Zachariae et al., 1996). The APC governs both mitotic progression and G1 maintenance via the binding of APC coactivators, Cdc20 and Cdh1, thereby allowing the timely degradation of cell cycle substrates (Peters, 2006). Remarkably, the core APC subunits are highly expressed in the mammalian brain, and Cdh1-APC operates in the nucleus of postmitotic neurons to regulate axon growth (Konishi et al., 2004; Lasorella et al., 2006; Stegmuller et al., 2006). However, the function of Cdc20-APC outside of the cell cycle in postmitotic cells has remained unexplored.

We report that Cdc20-APC is required for dendrite morphogenesis in mammalian neurons. Cdc20 is enriched at centrosomes in neurons, and this subcellular locus is critical for the ability of Cdc20-APC to drive dendrite development. We also forge an intimate biochemical and functional link between the centrosome-associated protein histone deacetylase 6 (HDAC6) and Cdc20-APC in neurons. Finally, we identify the centrosomally localized protein Id1 as a substrate of Cdc20-APC in neurons and demonstrate that Cdc20-APC-induced degradation of Id1 plays a critical role in dendrite development. These findings identify Cdc20-APC as the first ubiquitin ligase that specifies dendrite morphogenesis in the mammalian brain.

RESULTS

Cdc20 is required for dendrite morphogenesis in mammalian neurons

To investigate the role of Cdc20-APC in postmitotic neurons, we characterized the function of the key regulatory subunit Cdc20 in granule neurons of the rat cerebellar cortex. Granule neurons represent an ideal model for the study of neuronal morphogenesis and connectivity in the brain (Altman, 1972; Hatten and Heintz, 1995). Using four different antibodies, we found that Cdc20 protein is expressed in primary granule neurons (Figures 1A and S1A). Cdc20 protein levels increased with maturation, and introduction of small interfering RNAs targeting Cdc20 in granule neurons confirmed the specificity of the commercial antibody used throughout this study (Figures 1A and S1B). Finally, *in situ* hybridization of mouse cerebellar sections at P14 and P21 revealed Cdc20 mRNA expression in the internal granule layer (IGL) and Purkinje cell layer (Figure S1C). Together, these data indicate that Cdc20 is expressed in postmitotic neurons of the developing rodent cerebellar cortex. The time course of Cdc20 expression in primary neurons also suggested a possible role for Cdc20 in dendrite morphogenesis.

To interrogate Cdc20 function in neurons, we used a plasmid-based method of RNA interference (RNAi) to knockdown Cdc20 expression acutely. Expression of short hairpin RNAs (shRNAs) targeting two distinct regions of Cdc20 efficiently reduced the levels of exogenous and endogenous Cdc20 in heterologous cells and granule neurons, respectively (Figures 1B and S1D). Cdc20 knockdown in granule neurons led to a striking dendritic phenotype characterized by short primary dendrites (Figure 1C). Total dendrite length was reduced by approximately 65% relative to control transfected neurons (Figure 1D). Cdc20 knockdown did not affect cell survival, ruling out cell death as a cause of the Cdc20 RNAi-induced phenotype (Figure 1E). In addition, Cdc20 RNAi had little or no effect on axon length (Figure 1F). These results suggest that Cdc20 RNAi impairs the growth and development of dendrites.

We next performed a rescue experiment using an expression plasmid encoding an RNAi-resistant form of Cdc20 (Cdc20-RES) (Figure 1G). Expression of Cdc20 encoded by wild type

cDNA had little effect on the Cdc20 RNAi-induced dendritic phenotype (Figures 1H and 1I). In contrast, expression of Cdc20-RES in the background of Cdc20 RNAi restored dendrite arbor formation, increasing total dendrite length to 82% that of control transfected neurons (Figures 1H and 1I). These data indicate that the Cdc20 RNAi-induced loss of dendrites is the specific result of Cdc20 knockdown.

To determine if Cdc20's dendrite-promoting function is generalized in postmitotic neurons, we assessed the role of Cdc20 in cerebral cortical and hippocampal neurons. As with granule neurons, Cdc20 protein increased with maturation in cerebral cortical and hippocampal neurons (Figures S2A and S2B). Remarkably, in both populations of neurons, Cdc20 RNAi simplified the dendritic arbor, reducing the number of primary branches as well as secondary and tertiary dendritic branches, leading to dramatically reduced total dendrite length (Figures S2C-S2F). These results suggest that Cdc20 represents a generalized cell-intrinsic mechanism driving dendrite morphogenesis in mammalian neurons.

We next characterized the temporal dynamics of Cdc20 function in the development of dendrites. In cohort analyses of granule neurons transfected at a time prior to the generation of dendrites, Cdc20 RNAi flattened the dendrite growth curve (Figure S3A). In analyses in which neurons were transfected at a time when they already bear dendrites, Cdc20 knockdown triggered progressive shortening of dendrites (Figure S3B). Thus, Cdc20 promotes both the growth and maintenance of dendrites.

Time-lapse analyses of individual granule neurons revealed that dendrites display dynamic elongation and retraction during 48 hours of analysis in control neurons, which cumulatively led to increased total dendrite length (Figures S3C-S3G). However, dendrites in Cdc20 knockdown neurons often displayed retraction with little evidence of elongation, which cumulatively led to decreased total dendrite length (Figures S3C-S3G). Analyses of individual dendrites revealed similar results (Figures S3C and S3H-S3K). Collectively, these data demonstrate that Cdc20 supports the growth and maintenance of dendrites by promoting dendrite elongation and preventing dendrite retraction.

Cdc20 controls dendrite morphogenesis in vivo

Having demonstrated a dendritogenic function for Cdc20 in primary neurons, we next examined if Cdc20 is required for dendrite morphogenesis in the context of intact developing brain tissue. Using a biolistics method to trigger RNAi in rat organotypic cerebellar slices, we found that Cdc20 knockdown markedly inhibited the growth of primary dendrites and impaired dendritic arbor elaboration in granule neurons, leading to substantially reduced total dendrite length (Figures 2A and 2B). To determine the function of Cdc20 in the cerebellar cortex in vivo, we electroporated P3 rat pups with a Cdc20 RNAi plasmid that also encodes GFP (U6-cdc20i/CMV-GFP) or the corresponding control plasmid (U6/CMV-GFP). Animals were sacrificed at P8, and cerebella were subjected to immunohistochemical analyses using the GFP antibody. GFP-positive granule neurons were easily identifiable by their somal size and characteristic "T"-shaped parallel fiber (Figure 2C, left). Knockdown of Cdc20 by two distinct shRNAs in rat pups caused a marked dendritic deficit, characterized by shortened primary dendrites and a reduction in dendritic arbor complexity in IGL granule neurons (Figure 2C, right). Quantification of dendrites in IGL granule neurons revealed that Cdc20 RNAi substantially decreased total dendrite length to 40% that of granule neurons in control transfected animals (Figure 2D). Cdc20 knockdown had little or no effect on the health of granule neurons, parallel fiber patterning, or the number of parallel fibers associated with IGL granule neurons (Figure 2E and data not shown). Together, these findings suggest that Cdc20 is required for dendrite development in the cerebellar cortex in vivo.

Cdc20-APC operates at the centrosome to drive dendrite development

We next examined whether Cdc20's function in neurons is APC-dependent by assessing the role of the core APC subunit APC2 in dendrite morphogenesis (Peters, 2006). APC2 RNAi in granule neurons phenocopied the dendrite deficiency observed with Cdc20 RNAi (Figures 3A and S4A). As reported, Cdh1 knockdown did not affect dendrite growth (Figure 3A) (Konishi et al., 2004). These data suggest that Cdc20, but not Cdh1, functions in concert with the APC ubiquitin ligase to promote dendritic differentiation.

To gain further insight into the mechanism of Cdc20-APC function in dendrite development, we ascertained the subcellular location of Cdc20-APC in neurons. Subcellular fractionation of granule neurons revealed that Cdc20 resides predominantly in the cytoplasm, where a fraction of the APC core subunit Cdc27 is also present (Figure 3B). Immunofluorescence analyses confirmed that Cdc20 is expressed in granule neurons by co-staining for the neuron-specific class III β-tubulin Tuj1 (Figure 3C, right). Cdc20 exhibited diffuse, low intensity expression in the cytosol with marked concentration in a single perinuclear punctum, which was knocked down by Cdc20 RNAi, indicating that the punctate signal represents Cdc20-specific immunoreactivity (Figure 3C and S1D). Strikingly, Cdc20 tightly co-localized with the centrosomal markers γtubulin and pericentrin (Figures 3D and 3F). In contrast, neither an endoplasmic reticulum (protein disulphide isomerase (PDI)) nor a Golgi marker (GM130) co-localized with Cdc20 (Figure 3D). In corroborating biochemical analyses, centrosomal fractions isolated from granule neurons revealed that Cdc20 cofractionates with the centrosomal proteins γtubulin and 14-3-3ε (Figure 3E) (Pietromonaco et al., 1996). These data demonstrate that Cdc20 is enriched specifically at the centrosome in neurons.

We next evaluated the function of centrosomal Cdc20 in neurons. To localize Cdc20 at the centrosome, a sequence encoding 92 amino acids of the PACT domain from AKAP450 was inserted N-terminal to the RNAi-resistant Cdc20-RES cDNA (PACT-Cdc20-RES) (Gillingham and Munro, 2000). Since a pool of Cdc20 was observed in the nucleus of neurons (Figure 3B), a nuclearly targeted Cdc20-RES expression plasmid was also generated (NLS-Cdc20-RES). We confirmed the proper nuclear and centrosomal localization of NLS-Cdc20-RES and PACT-Cdc20-RES, respectively, in cells and neurons (Figures S5A and 3F). Nuclear Cdc20-RES failed to rescue the Cdc20 RNAi dendrite phenotype in granule neurons in primary dissociated and organotypic cerebellar cultures (Figures 3G, 3H, and S6A). In contrast, centrosomal Cdc20-RES completely reversed the dendritic impairment induced by Cdc20 RNAi in both settings (Figures 3G, 3H, and S6A). Neither the PACT domain alone nor a PACT domain-Cdh1 fusion protein restored dendrite length in the background of Cdc20 RNAi (Figure 3G), indicating that centrosomal Cdc20, and not the PACT domain itself, promotes dendritic morphogenesis. Together, these data suggest that localizing neuronal Cdc20-APC to the centrosome drives dendrite morphogenesis.

We next determined if the centrosomal localization of Cdc20 is required for its ability to promote dendrite development. Deletion of the N-terminal domain of Cdc20 (amino acids 1–167) disrupted the centrosomal concentration of Cdc20 in neurons, consistent with results in nonneural cells (Figures 4A and 4B) (Kallio et al., 2002). Further analysis of the N-terminal domain of Cdc20 revealed a requirement for a 57 amino acid region (111–167) in concentrating Cdc20 at the centrosome (Figures 4A, 4B, and S5B). A Cdc20-RES mutant in which the 57 amino acid region is deleted (Cdc20Δ111-167-RES) failed to reverse the Cdc20 RNAi-induced dendrite loss (Figures 4C and 4D). Fusion of the PACT domain to Cdc20Δ111-167-RES restored the ability of the mutant Cdc20-RES to stimulate dendrite development in the background of Cdc20 RNAi, suggesting that this 57 amino acid region of Cdc20 harbors a centrosomal localization signal (CLS) (Figures 4E and S5C). Finer deletions of the 57 amino acid region revealed a requirement for a short 19 amino acid motif (111–129) for both the centrosomal localization of Cdc20 and Cdc20-induced dendrite elaboration (Figures 4F-4H,

S5D, and S5E). Fusion of the PACT domain to Cdc20Δ111-129-RES restored the ability of the mutant Cdc20-RES to stimulate dendrite development, suggesting that the function of amino acids 111–129 is to provide a CLS (data not shown). Collectively, our results establish that centrosomal localization of Cdc20 is essential for the ability of Cdc20 to promote dendrite morphogenesis.

HDAC6 promotes Cdc20 function in neurons

We next investigated how Cdc20-APC is controlled at the centrosome in neurons. The class IIb histone deacetylase HDAC6 localizes to the basal body, a centrosome-derived organelle, and may regulate primary ciliary morphogenesis (Pugacheva et al., 2007). In addition to its two N-terminal deacetylase domains, HDAC6 harbors a C-terminal zinc finger ubiquitin-binding domain, ZnF-UBP (Seigneurin-Berny et al., 2001). Because of its localization, involvement in ubiquitin signaling, and function in cellular morphogenesis, we asked whether HDAC6 plays a role in the control of Cdc20-APC function in dendrite development.

We first assessed whether HDAC6 interacts with Cdc20 in cells. HDAC6 associated with Cdc20 in transfected cells (Figure 5A). Biochemical and immunofluorescence studies verified that HDAC6 resides in neuronal centrosomes (Figure 5B and data not shown). Accordingly, HDAC6 interacted with Cdc20 endogenously in neurons (Figure 5C). In other analyses, we found that the C-terminal region of Cdc20 (amino acids 311–499) interacted with HDAC6 (Figure S7A). A Cdc20-RES mutant lacking the HDAC6-interacting region (Cdc20-1-310-RES) failed to restore dendrite length in the background of Cdc20 RNAi, suggesting that the physical interaction of Cdc20 with HDAC6 is critical for Cdc20-dependent dendrite development (Figures S7A and S7B).

To determine if HDAC6 influences Cdc20-APC activity, we devised a cell-based degradation assay to monitor changes in centrosomal Cdc20-APC activity. We designed an expression plasmid encoding the first 88 amino acids of the mitotic Cdc20-APC substrate securin fused to firefly luciferase. This segment of securin contains the destruction box (D-box), an APC degron (Zur and Brandeis, 2001). We used the PACT domain to localize the degradation reporter to the centrosome (Figure 5D). A mutation in the securin D-box was introduced into the reporter to serve as a control. Cdc20 knockdown caused an increase in relative levels of the securin-luciferase reporter in neurons, demonstrating that this assay represents a valid readout for centrosomal Cdc20-APC activity (Figure 5D). Importantly, HDAC6 RNAi in granule neurons also increased the relative abundance of the securin-luciferase reporter (Figure 5D). In control experiments, expression of HDAC6 shRNA induced knockdown of exogenous as well as endogenous HDAC6 in cells (Figure 5E). These data suggest that endogenous HDAC6 promotes Cdc20-APC activity at the centrosome in neurons.

We next determined whether endogenous HDAC6 is relevant to dendrite morphogenesis. HDAC6 knockdown using two different shRNAs in granule neurons markedly reduced dendrite elaboration and decreased total dendrite length (Figure 5F and data not shown). HDAC6 RNAi also disrupted the formation of the granule neuron dendritic arbor in the cerebellar cortex in slices and in rat pups in vivo (Figures S6B and 5G). Further, knockdown of HDAC6 in hippocampal neurons decreased total dendrite length and reduced dendritic branching, suggesting that HDAC6 has a generalized dendritogenic function in mammalian neurons (Figures S8A and S8B). Together, these data indicate that HDAC6 knockdown phenocopies the effect of Cdc20 RNAi in neurons. In epistasis experiments in granule neurons, we found that overexpression of HDAC6 stimulated dendrite elaboration, an effect suppressed by Cdc20 RNAi, suggesting that HDAC6 promotes dendrite elaboration in a Cdc20-dependent manner (Figure 5H). Collectively, our findings suggest that HDAC6 promotes the activity of centrosomal Cdc20-APC and thereby drives dendrite morphogenesis.

HDAC6 promotes Cdc20 polyubiquitination

We next determined the molecular basis underlying the ability of HDAC6 to stimulate neuronal Cdc20-APC activity and function. HDAC6 knockdown did not appear to alter the centrosomal localization of Cdc20 or centrosomal structure in neurons (Figures S9A and S9B). Because HDAC6 harbors deacetylase activity, we examined the effect of HDAC6 on the acetylation status of Cdc20 but detected no appreciable change in Cdc20 acetylation upon manipulation of HDAC6 levels (data not shown). Recent evidence suggests that autoubiquitination of Cdc20 leads to increased Cdc20-APC activity in cycling cells (Reddy et al., 2007; Stegmeier et al., 2007). In addition, HDAC6 may stabilize polyubiquitinated proteins via its C-terminal ZnF-UBP domain (Boyault et al., 2006). These observations raised the question of whether HDAC6, through its ZnF-UBP domain, might promote the polyubiquitination of Cdc20, thereby activating Cdc20-APC.

Expression of wild type HDAC6 robustly increased the polyubiquitination of co-expressed Cdc20 in cells (Figure 6A). Likewise, expression of an HDAC6 mutant deficient in deacetylase activity (HDAC6(DM)) increased Cdc20 ubiquitination (Figure 6A). Importantly, an HDAC6 mutant lacking the ZnF-UBP domain (HDAC(ΔC)) did not augment Cdc20 ubiquitination, suggesting that the ZnF-UBP domain but not the deacetylase activity of HDAC6 is required to increase Cdc20 polyubiquitination (Figure 6A). In in vitro ubiquitination experiments, addition of full-length HDAC6 but not HDAC6(ΔC) markedly promoted Cdc20 ubiquitination (Figure S10A). However, the HDAC6 ZnF-UBP domain was dispensable for Cdc20 binding in vitro (Figure S10B). These results suggest that HDAC6 directly binds Cdc20 and subsequently stimulates Cdc20-APC activity via ZnF-UBP domain-dependent stabilization of Cdc20 polyubiquitination. In agreement with the results in heterologous cells and in vitro, we found that the ubiquitination of neuronal Cdc20 was robustly reduced by HDAC6 knockdown (Figure 6B).

The requirement of the HDAC6 ZnF-UBP domain in promoting Cdc20 polyubiquitination would predict that the ZnF-UBP domain is critical for the ability of HDAC6 to promote dendrite development. To test this prediction, we performed structure-function analyses of an RNAi-resistant form of HDAC6 (HDAC6-RES) in the background of HDAC6 RNAi in neurons (Figure 6C). Expression of HDAC6-RES or deacetylase-deficient HDAC6-RES effectively reversed the HDAC6 RNAi-induced dendrite deficit (Figures 6D and 6E). However, an HDAC6-RES mutant lacking the ZnF-UBP domain failed to rescue the HDAC6 RNAi-induced dendrite phenotype, suggesting that HDAC6 promotes the elaboration of dendrites through the ZnF-UBP domain (Figures 6D and 6E). Together, our results suggest that HDAC6 via its ZnF-UBP domain promotes Cdc20 polyubiquitination, stimulates Cdc20-APC activity, and drives dendrite morphogenesis.

Recent studies have employed the Cdc20-specific deubiquitinase USP44 to demonstrate that Cdc20 polyubiquitination stimulates Cdc20-APC activity in dividing cells (Stegmeier et al., 2007). The USP44 gene is expressed in neurons, including granule neurons of the rodent cerebellar cortex (http://mouse.brain-map.org and data not shown). Knockdown of USP44 in neurons dramatically increased the polyubiquitination of Cdc20 and centrosomal Cdc20-APC activity, confirming that endogenous USP44 deubiquitinates Cdc20 in neurons (Figures 6F, 6G, and 6I). USP44 knockdown substantially increased dendrite length and branching in cerebellar granule neurons and hippocampal neurons, suggesting that Cdc20 deubiquitination restrains dendrite development (Figures 6H, S8C and S8D). In epistasis experiments, Cdc20 RNAi suppressed the USP44 RNAi-induced increase in dendrite length, suggesting that USP44 knockdown stimulates dendrite development in a Cdc20-dependent manner (Figures 6J). Together, these results suggest that the polyubiquitination of endogenous Cdc20 plays a critical role in Cdc20-dependent dendrite morphogenesis.

Cdc20-APC triggers degradation of the centrosomal protein Id1

A major question that remained to be addressed is how centrosomal Cdc20-APC promotes dendrite development. We reasoned that Cdc20-APC might stimulate the ubiquitination and consequent degradation of a centrosomally localized protein that inhibits dendrite growth. Interrogation of the literature for proteins that are localized at the centrosome and harbor a conserved Cdc20-recognition D-box motif revealed that the helix-loop-helix protein Id1 fulfills both criteria (Figure S11A, top) (Hasskarl et al., 2004). We confirmed that Id1 resides at the centrosome in granule neurons (Figures 7A and 7B). Exposure of neurons to the proteasome inhibitor MG132 substantially increased Id1 levels, suggesting that Id1 is regulated by the ubiquitin-proteasome system in neurons (Figure 7C). Expression of Id1 declined in granule neurons with maturation, inversely correlating with increasing Cdc20 protein expression, suggesting that Cdc20 might regulate Id1 abundance in neurons (Figure 7D). Consistent with this possibility, Cdc20 and Id1 formed a physical complex in a D-box-dependent manner in cells (Figure S11A, bottom). Cdc20-APC directly catalyzed the ubiquitination of Id1 in vitro, suggesting that Id1 is a substrate of Cdc20-APC (Figure 7E). Importantly, Cdc20 knockdown triggered the accumulation of endogenous Id1 protein in neurons (Figure 7F). Collectively, these results identify the centrosomally localized protein Id1 as a novel substrate of neuronal Cdc20-APC.

We next characterized the function of Id1 in neurons. Id1 knockdown using two different shRNAs markedly increased dendrite length in granule neurons (Figures 7G, S11B, and S11C). Importantly, Id1 RNAi-induced dendrite growth was specifically reversed by expression of an RNAi-resistant form of Id1 (Figures 7H, S11D, and S11E). We also found that Id1 knockdown in the cerebellar cortex in vivo led to more elaborate dendritic arbors with increased total dendrite length in IGL granule neurons (Figure 7I). Knockdown of Id1 in primary hippocampal neurons also stimulated dendrite growth and branching, suggesting a generalized inhibitory role for Id1 in dendrite morphogenesis in mammalian neurons (Figures S8E and S8F).

In epistasis experiments, the combination of Id1 RNAi and Cdc20 RNAi led to increased total dendrite length that was indistinguishable from that of Id1 RNAi alone, suggesting that Id1 lies functionally downstream of Cdc20 (Figure 7J). In gain-of-function analyses of Id1, expression of a mutant Id1 protein in which the D-box motif was mutated substantially reduced dendrite length (Figure S11F). These results suggest that Cdc20-APC-induced degradation of the centrosomal protein Id1 plays a critical role in promoting dendrite growth and branching. Collectively, we have elucidated a novel centrosomal Cdc20-APC ubiquitin ligase pathway that governs dendrite morphogenesis in the mammalian brain (see model in Figure 7K).

DISCUSSION

In this study, we have discovered a centrosomal Cdc20-APC ubiquitin signaling pathway that plays a fundamental role in dendrite morphogenesis in the mammalian brain. The ubiquitin ligase Cdc20-APC has received wide attention for its essential function in driving the metaphase-anaphase transition in cycling cells (Peters, 2006). Our study reveals a novel postmitotic function for this mitotic ubiquitin ligase and suggests that the mitotic machinery may play widespread roles in unique aspects of neural development.

The dendrite-promoting effect of Cdc20-APC provides an interesting counterpoint to the axon-specific regulatory effect of Cdh1-APC (Konishi et al., 2004). Whereas Cdh1-APC functions in the nucleus in neurons to control axon growth and patterning (Konishi et al., 2004; Lasorella et al., 2006; Stegmuller et al., 2006), Cdc20-APC operates at the centrosome to drive dendrite morphogenesis through the promotion of both dendrite growth and maintenance. Thus, the APC may act as a pivotal regulator of neuronal morphogenesis through specific recruitment of the coactivators Cdc20 and Cdh1 in distinct subcellular compartments.

Elucidation of the centrosomal HDAC6/Cdc20-APC signaling cassette implies that both HDAC6 and Cdc20-APC may exert novel functions beyond the control of dendrite morphogenesis. HDAC6 localized to the centrosome-derived basal body has been implicated in the control of primary cilium stability in epithelial cells (Pugacheva et al., 2007). Although the role of the ZnF-UBP domain of HDAC6 in ciliary biology remains undefined, identification of the intimate centrosomal HDAC6/Cdc20-APC link raises the possibility that centrosomal Cdc20-APC also operates outside the cell cycle in epithelial cells to control the morphology of the primary cilium. This scenario raises intriguing parallels between the biology of primary cilia in epithelial cells and dendrite development in neurons.

The identification of Cdc20-APC as the first E3 ubiquitin ligase that specifically regulates the growth and elaboration of dendrites in mammalian neurons has important ramifications for our understanding of the cell-intrinsic control of neuronal morphology and circuitry. Genetic studies in fly and mammalian neurons have highlighted the importance of transcription factors in diverse aspects of the cell-intrinsic control of dendrite morphogenesis, including growth, branching, and cell type-specific arborization (Parrish et al., 2007). In future studies, it will be important to determine how the activities of centrosomal Cdc20-APC and transcription factors are integrated in the specification and elaboration of dendrites. Another line of inquiry should address how Cdc20-APC controls the effects of extrinsic cues on dendrite morphogenesis in the developing brain. Beyond dendrite growth and elaboration, it will be interesting to determine if the centrosomal Cdc20-APC pathway might contribute to dendritic refinement and plasticity.

The identification of Id1 as a substrate of neuronal Cdc20-APC provides important clues as to how Cdc20-APC regulates dendrite morphogenesis. Since Id1 localizes at the centrosome but does not likely represent an integral component of the centrosome, our findings suggest that the centrosome acts as a signaling platform for the Cdc20-APC ubiquitin ligase pathway in the control of dendrite development. In agreement with this conclusion, Cdc20 knockdown does not appear to disrupt the structure of the centrosome as assessed by expression of the centrosomal proteins pericentrin and γtubulin (Figure S12). How the Id1 signal from its centrosomal locale is coupled to the regulation of dendrites is an important question for future studies. Whether additional centrosomal substrates of neuronal Cdc20-APC regulate dendrite morphogenesis also remains to be addressed.

During brain development, centrosomes have been demonstrated to function in neuronal migration as well as axonal specification and growth (Higginbotham and Gleeson, 2007). Our finding that Cdc20-APC operates from a centrosomal locus to specify the growth and elaboration of dendrites highlights a connection between centrosomal biology and dendrite morphogenesis. The centrosomal proteins LIS1 and DISC1, implicated in lissencephaly and schizophrenia respectively, play roles in dendritic development (Duan et al., 2007; Liu et al., 2000). Thus, the centrosome in postmitotic neurons may represent a critical signaling platform for dendritogenic pathways, and the deregulation of these pathways may contribute to the pathogenesis of neurological and psychiatric disorders.

EXPERIMENTAL PROCEDURES

Primary neuron cultures and transfection

Primary cerebellar granule neurons were prepared from P6 rat pups and transfected using a modified calcium phosphate method as described (Konishi et al., 2004). Granule neurons are postmitotic at the time of transfection as they fail to incorporate bromo-deoxyuridine (Konishi and Bonni, 2003). To avoid the possibility that the morphological effects of RNAi or protein expression were due to any effect of these manipulations on cell survival, a plasmid encoding the anti-apoptotic protein Bcl-X_L was included in all neuronal transfections except those in

which survival was assessed. Expression of Bcl-X_L had little or no effect on dendritic or axonal morphology as reported (Gaudilliere et al., 2004; Konishi et al., 2004). In additional experiments, granule neurons were transfected with the Cdc20, HDAC6, USP44, Id1, or control U6 RNAi plasmid along with a GFP expression plasmid in the absence of Bcl-X_L (Figure S13). In all cases, the dendrite phenotypes observed in the presence of Bcl-X_L paralleled exactly the dendrite effects observed without Bcl-X_L (Figure S13).

Hippocampal and cerebral cortical neuron cultures were prepared from rat embryos (embryonic day 18) as described (Goslin et al., 1998). Neurons were plated on poly-L-lysine-coated in Neurobasal medium plus B-27 (Invitrogen). Transfections were performed on DIV 1.

Cerebellar slice cultures and in vivo electroporation

P6-P9 rat cerebella were dissected for organotypic slice cultures and transfected as described (Gaudilliere et al., 2004; Shalizi et al., 2006). In vivo electroporation of P3 Sprague-Dawley rat pups was performed as described (Konishi et al., 2004).

Immunocytochemistry

For visualization of centrosomal proteins, cells were fixed in methanol for 10 min at −20° and subjected to immunofluorescence analysis with the indicated antibodies using standard protocols. For other immunocytochemistry experiments, cells were fixed in 4% paraformaldehyde for 20 minutes at room temperature.

Subcellular fractionation and centrosome isolation

Subcellular fractionation into cytosolic and nuclear fractions was performed as described (Konishi et al., 2004). Centrosomal fractions were isolated as described (Bornens et al., 1987).

In vitro Cdc20-APC-mediated ubiquitination

Ubiquitination of in vitro translated substrate by Cdc20-APC was performed as described (Konishi et al., 2004; Rape and Kirschner, 2004). Lysates of HeLa cells arrested in early mitosis were prepared. After addition of (1:1) APC lysis buffer (1% Triton X-100, 150 mM NaCl, 50 mM Tris pH 7.2, and 2mM EDTA, and 1 mM DTT plus protease inhibitor cocktail and NaF), the APC was immunoprecipitated using a mouse Cdc27 antibody (Santa Cruz) followed by protein G-sepharose. Immunoprecipitates were washed once with the APC lysis buffer followed by two washes with hypotonic lysis buffer (SB). In vitro ubiquitination was performed by incubation of APC and eluted FLAG-Cdc20 with ^{35}S-Met-labeled, in vitro translated myc-Id1 for 1 hr at 37 °C in a reaction mix consisting of 5 mM Tris pH 7.5, 1 mM $MgCl_2$, 2 mM ATP, 0.1 mM EGTA, 30 U/ml creatine phosphokinase, 7.5 mM phosphocreatine, and 2 μM ubiquitin aldehyde together with 12.5 μg ubiquitin, 400 ng ubiquitin-activating enzyme (E1), and 500 ng UbcH10 (Boston Biochem). Reaction products were resolved by SDS-PAGE followed by nitrocellulose transfer. Radioactivity was visualized by Phosphorimager analysis.

Analysis of neuronal morphology

The axonal and dendritic morphology of granule neurons in culture, in cerebellar slices, and in vivo were analyzed in a blinded fashion using a Nikon Eclipse TE2000 epifluorescence microscope to capture images. SPOT software was used to measure process length.

Statistics

Analyses were performed using Statview 5.0.1 software. All histogram data are presented as mean + SEM unless otherwise specified. The t-test was used for comparisons in experiments with only two groups. In experiments with more than two groups, analysis of variance

(ANOVA) was performed followed by Fisher's Least Significant Difference or the Bonferroni test for pairwise comparisons among three and greater than three groups, respectively. For analysis of more than two groups of non-parametric data, the Kruskal-Wallis test was used.

Supplementary Material

Refer to Web version on PubMed Central for supplementary material.

Acknowledgments

Supported by NIH grants NS051255 and NS41021 (AB), a Ruth L. Kirschstein NRSA research fellowship, NCI, and Brain Science Foundation grant (AHK), the Albert J Ryan Foundation (PB), and a Human Frontier Science Program grant (YI). We thank members of the Bonni laboratory for helpful discussions and critical reading of the manuscript.

References

Altman J. Postnatal development of the cerebellar cortex in the rat. 3. Maturation of the components of the granular layer. J Comp Neurol 1972;145:465–513. [PubMed: 4114591]

Becker EB, Bonni A. Beyond proliferation-cell cycle control of neuronal survival and differentiation in the developing mammalian brain. Semin Cell Dev Biol 2005;16:439–448. [PubMed: 15840451]

Bornens M, Paintrand M, Berges J, Marty MC, Karsenti E. Structural and chemical characterization of isolated centrosomes. Cell Motil Cytoskeleton 1987;8:238–249. [PubMed: 3690689]

Boyault C, Gilquin B, Zhang Y, Rybin V, Garman E, Meyer-Klaucke W, Matthias P, Muller CW, Khochbin S. HDAC6-p97/VCP controlled polyubiquitin chain turnover. Embo J 2006;25:3357–3366. [PubMed: 16810319]

Duan X, Chang JH, Ge S, Faulkner RL, Kim JY, Kitabatake Y, Liu XB, Yang CH, Jordan JD, Ma DK, et al. Disrupted-In-Schizophrenia 1 regulates integration of newly generated neurons in the adult brain. Cell 2007;130:1146–1158. [PubMed: 17825401]

Gaudilliere B, Konishi Y, de la Iglesia N, Yao G, Bonni A. A CaMKII-NeuroD signaling pathway specifies dendritic morphogenesis. Neuron 2004;41:229–241. [PubMed: 14741104]

Gillingham AK, Munro S. The PACT domain, a conserved centrosomal targeting motif in the coiled-coil proteins AKAP450 and pericentrin. EMBO Rep 2000;1:524–529. [PubMed: 11263498]

Goslin, K.; Asmussen, H.; Banker, GA. Rat Hippocampal Neurons in Low-Density Culture. Vol. 2. Cambridge, MA; MIT Press: 1998.

Greene LA, Biswas SC, Liu DX. Cell cycle molecules and vertebrate neuron death: E2F at the hub. Cell Death Differ 2004;11:49–60. [PubMed: 14647236]

Hasskarl J, Duensing S, Manuel E, Munger K. The helix-loop-helix protein ID1 localizes to centrosomes and rapidly induces abnormal centrosome numbers. Oncogene 2004;23:1930–1938. [PubMed: 14755252]

Hatten ME, Heintz N. Mechanisms of neural patterning and specification in the developing cerebellum. Annu Rev Neurosci 1995;18:385–408. [PubMed: 7605067]

Higginbotham HR, Gleeson JG. The centrosome in neuronal development. Trends in neurosciences 2007;30:276–283. [PubMed: 17420058]

Kallio MJ, Beardmore VA, Weinstein J, Gorbsky GJ. Rapid microtubule-independent dynamics of Cdc20 at kinetochores and centrosomes in mammalian cells. The Journal of cell biology 2002;158:841–847. [PubMed: 12196507]

Kaufmann WE, Moser HW. Dendritic anomalies in disorders associated with mental retardation. Cereb Cortex 2000;10:981–991. [PubMed: 11007549]

King RW, Peters JM, Tugendreich S, Rolfe M, Hieter P, Kirschner MW. A 20S complex containing CDC27 and CDC16 catalyzes the mitosis-specific conjugation of ubiquitin to cyclin B. Cell 1995;81:279–288. [PubMed: 7736580]

Knobloch M, Mansuy IM. Dendritic spine loss and synaptic alterations in Alzheimer's disease. Molecular neurobiology 2008;37:73–82. [PubMed: 18438727]

Konishi Y, Bonni A. The E2F-Cdc2 cell-cycle pathway specifically mediates activity deprivation-induced apoptosis of postmitotic neurons. J Neurosci 2003;23:1649–1658. [PubMed: 12629169]

Konishi Y, Stegmuller J, Matsuda T, Bonni S, Bonni A. Cdh1-APC controls axonal growth and patterning in the mammalian brain. Science 2004;303:1026–1030. [PubMed: 14716021]

Lasorella A, Stegmuller J, Guardavaccaro D, Liu G, Carro MS, Rothschild G, de la Torre-Ubieta L, Pagano M, Bonni A, Iavarone A. Degradation of Id2 by the anaphase-promoting complex couples cell cycle exit and axonal growth. Nature 2006;442:471–474. [PubMed: 16810178]

Liu Z, Steward R, Luo L. Drosophila Lis1 is required for neuroblast proliferation, dendritic elaboration and axonal transport. Nat Cell Biol 2000;2:776–783. [PubMed: 11056531]

Parrish JZ, Emoto K, Kim MD, Jan YN. Mechanisms that regulate establishment, maintenance, and remodeling of dendritic fields. Annu Rev Neurosci 2007;30:399–423. [PubMed: 17378766]

Peters JM. The anaphase promoting complex/cyclosome: a machine designed to destroy. Nat Rev Mol Cell Biol 2006;7:644–656. [PubMed: 16896351]

Pietromonaco SF, Seluja GA, Aitken A, Elias L. Association of 14-3-3 proteins with centrosomes. Blood Cells Mol Dis 1996;22:225–237. [PubMed: 9075573]

Pugacheva EN, Jablonski SA, Hartman TR, Henske EP, Golemis EA. HEF1-dependent Aurora A activation induces disassembly of the primary cilium. Cell 2007;129:1351–1363. [PubMed: 17604723]

Rape M, Kirschner MW. Autonomous regulation of the anaphase-promoting complex couples mitosis to S-phase entry. Nature 2004;432:588–595. [PubMed: 15558010]

Reddy SK, Rape M, Margansky WA, Kirschner MW. Ubiquitination by the anaphase-promoting complex drives spindle checkpoint inactivation. Nature 2007;446:921–925. [PubMed: 17443186]

Seigneurin-Berny D, Verdel A, Curtet S, Lemercier C, Garin J, Rousseaux S, Khochbin S. Identification of components of the murine histone deacetylase 6 complex: link between acetylation and ubiquitination signaling pathways. Mol Cell Biol 2001;21:8035–8044. [PubMed: 11689694]

Shalizi A, Gaudilliere B, Yuan Z, Stegmuller J, Shirogane T, Ge Q, Tan Y, Schulman B, Harper JW, Bonni A. A calcium-regulated MEF2 sumoylation switch controls postsynaptic differentiation. Science 2006;311:1012–1017. [PubMed: 16484498]

Stegmeier F, Rape M, Draviam VM, Nalepa G, Sowa ME, Ang XL, McDonald ER 3rd, Li MZ, Hannon GJ, Sorger PK, et al. Anaphase initiation is regulated by antagonistic ubiquitination and deubiquitination activities. Nature 2007;446:876–881. [PubMed: 17443180]

Stegmuller J, Konishi Y, Huynh MA, Yuan Z, Dibacco S, Bonni A. Cell-intrinsic regulation of axonal morphogenesis by the Cdh1-APC target SnoN. Neuron 2006;50:389–400. [PubMed: 16675394]

Zachariae W, Shin TH, Galova M, Obermaier B, Nasmyth K. Identification of subunits of the anaphase-promoting complex of Saccharomyces cerevisiae. Science 1996;274:1201–1204. [PubMed: 8895471]

Zur A, Brandeis M. Securin degradation is mediated by fzy and fzr, and is required for complete chromatid separation but not for cytokinesis. Embo J 2001;20:792–801. [PubMed: 11179223]

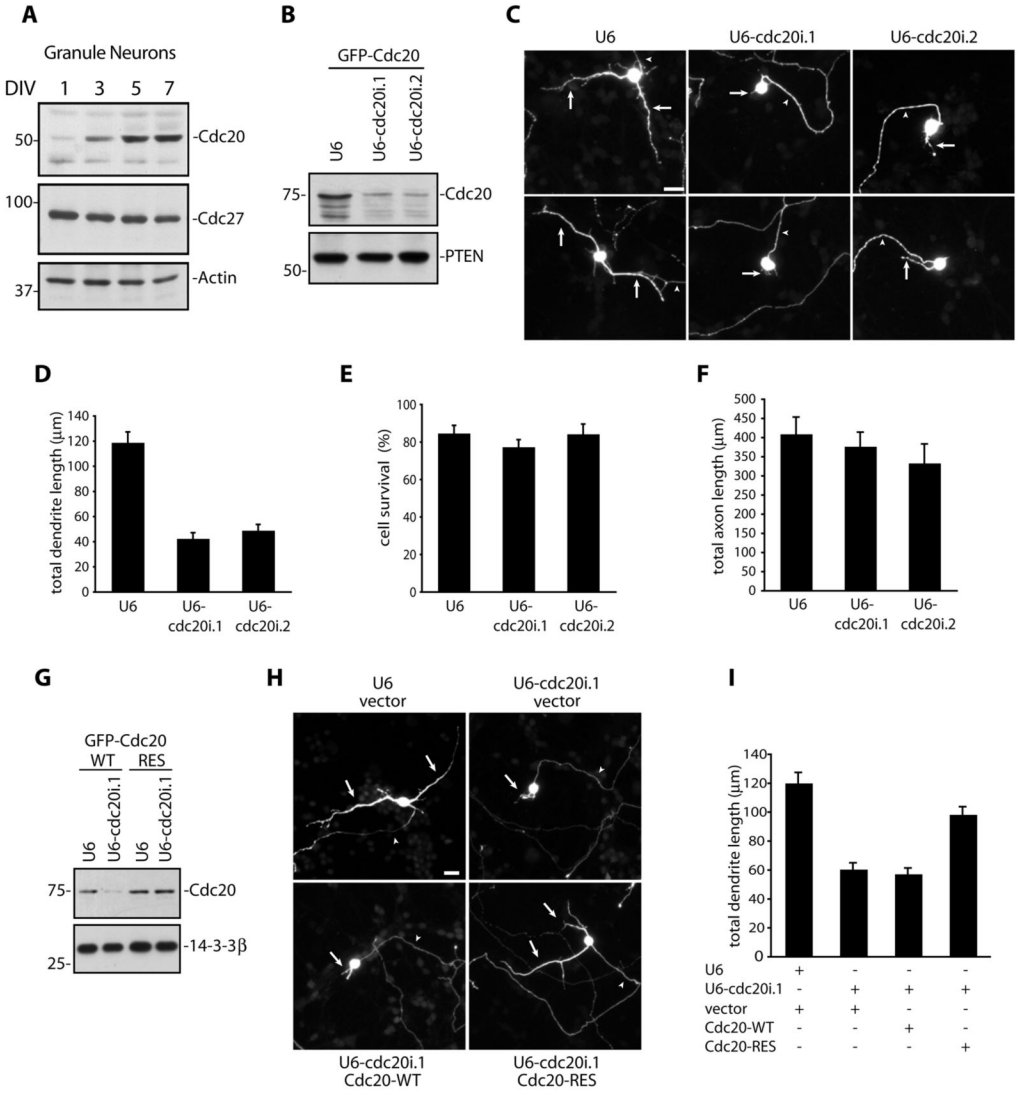

Figure 1. Cdc20 is required for dendrite development

(A) Lysates from primary cerebellar granule neurons were immunoblotted with the indicated antibodies. DIV = days in vitro. **(B)** Lysates from COS cells transfected with the expression plasmid encoding GFP-Cdc20 together with one of two Cdc20 RNAi plasmids or control U6 plasmid were immunoblotted with the indicated antibodies. **(C)** Granule neurons transfected with a Cdc20 RNAi or control U6 plasmid together with a GFP expression plasmid were subjected to immunocytochemistry using the GFP antibody four days after transfection. Representative neurons are shown. In all images of neuronal morphology, arrows and arrowheads indicate dendrites and axons, respectively. Bar = 10 μm. **(D)** Total dendrite length from granule neurons treated as in (C) was quantified and is presented as mean + SEM. Dendrite length was significantly lower in Cdc20 knockdown neurons compared to control U6-transfected neurons (ANOVA; $P < 0.0001$). 388 neurons were measured. **(E)** Granule neurons were transfected with a Cdc20 RNAi or control U6 plasmid together with a β-galactosidase expression plasmid and subjected to immunocytochemistry using the β-galactosidase antibody and the DNA dye bisbenzamide (Hoechst 33258). Cell survival was scored by assessment of process fragmentation and nuclear condensation. **(F)** Granule neurons were transfected and analyzed as in (C). Total axon length was not significantly different in Cdc20 knockdown and

control U6-transfected neurons. 340 neurons were measured. **(G)** Lysates of COS cells transfected with the GFP-Cdc20-WT or GFP-Cdc20-RES expression plasmid along with the Cdc20 RNAi or control U6 plasmid were immunoblotted with the indicated antibodies. **(H)** Granule neurons transfected with the Cdc20 RNAi or control U6 plasmid together with the expression plasmid encoding Cdc20-WT, Cdc20-RES, or control vector were analyzed as in Figure 1C. Bar = 10 μm. **(I)** Neurons treated as in (H) were quantified for total dendrite length. Cdc20-RES but not Cdc20-WT significantly increased dendrite length in the background of Cdc20 RNAi (ANOVA; $P < 0.0001$). 630 neurons were measured.

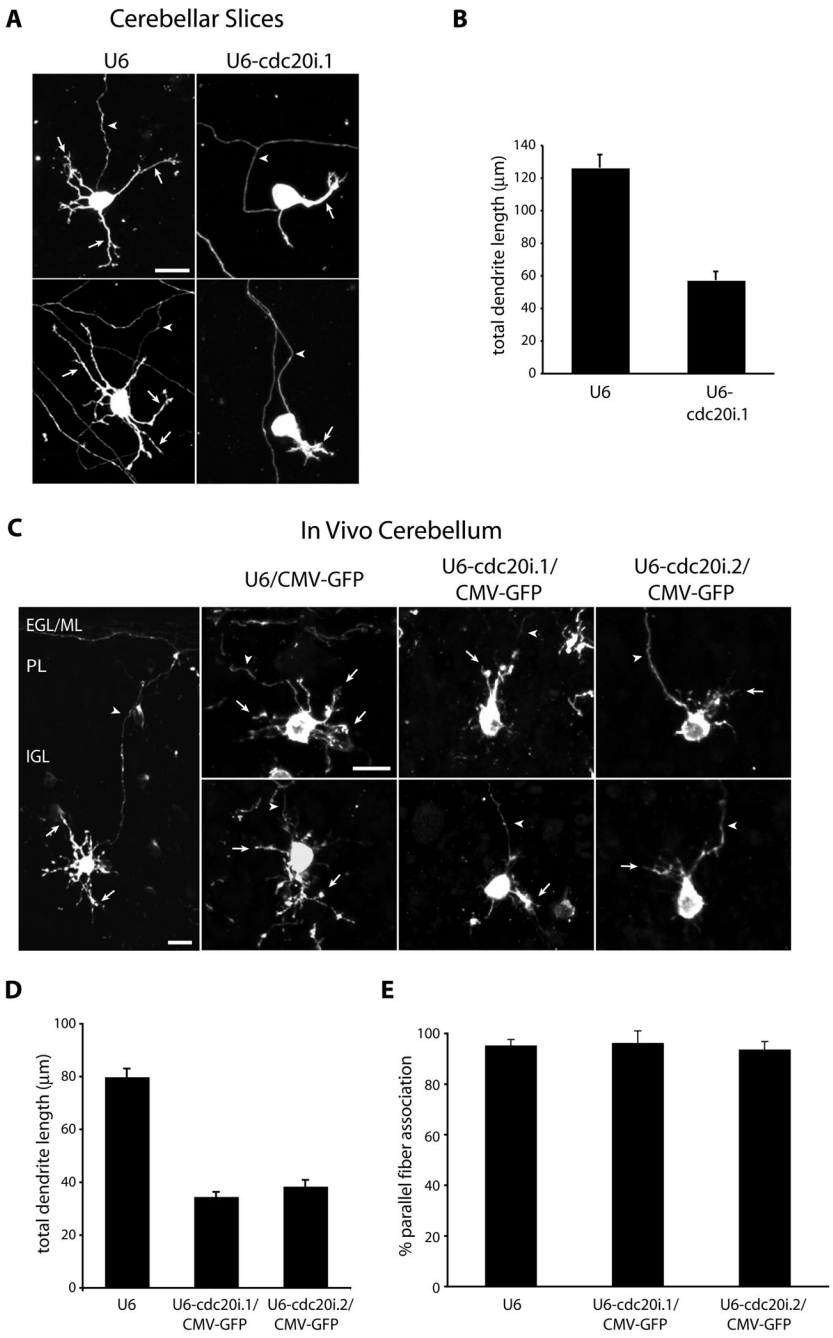

Figure 2. Cdc20 promotes dendrite development in cerebellar slices and in vivo

(A) Rat cerebellar slices transfected by a biolistics method with the Cdc20 RNAi or control U6 plasmid together with the GFP expression plasmid were subjected to immunohistochemistry four days after transfection using the GFP antibody. Representative granule neurons are shown. Bar = 10 μm. **(B)** Total dendrite length in transfected IGL granule neurons in slices analyzed as in (A) was measured. Cdc20 knockdown neurons had significantly shorter dendrites compared to control U6-transfected neurons (t-test; $P < 0.0001$). 130 neurons were measured. **(C)** Rat pups electroporated in vivo with a U6-cdc20i/CMV-GFP RNAi or control U6/CMV-GFP plasmid were sacrificed five days after electroporation, and cerebella were subjected to immunohistochemistry using the GFP antibody. Left panel: A typical control

U6-transfected granule neuron is shown with its soma and dendrites (arrows) in the internal granule layer (IGL) and an ascending axon (arrowhead) connecting to a horizontally oriented parallel fiber above. Right panels: Representative neurons for each condition are shown. EGL/ML = external granule and molecular layers. PL = Purkinje cell layer. Bar = 10 μm. **(D)** Total dendrite length following in vivo electroporation as in (C) was quantified in transfected IGL granule neurons. Cdc20 RNAi significantly reduced granule neuron dendrite length compared to control (ANOVA; $P < 0.0001$). 251 neurons were measured. **(E)** Transfected granule neurons were counted in the IGL and axons were counted in the molecular layer as described (Stegmuller et al., 2006). No significant differences in parallel fiber number were observed in animals transfected with the Cdc20 RNAi plasmids compared to control U6 transfected animals. 668 neurons were measured.

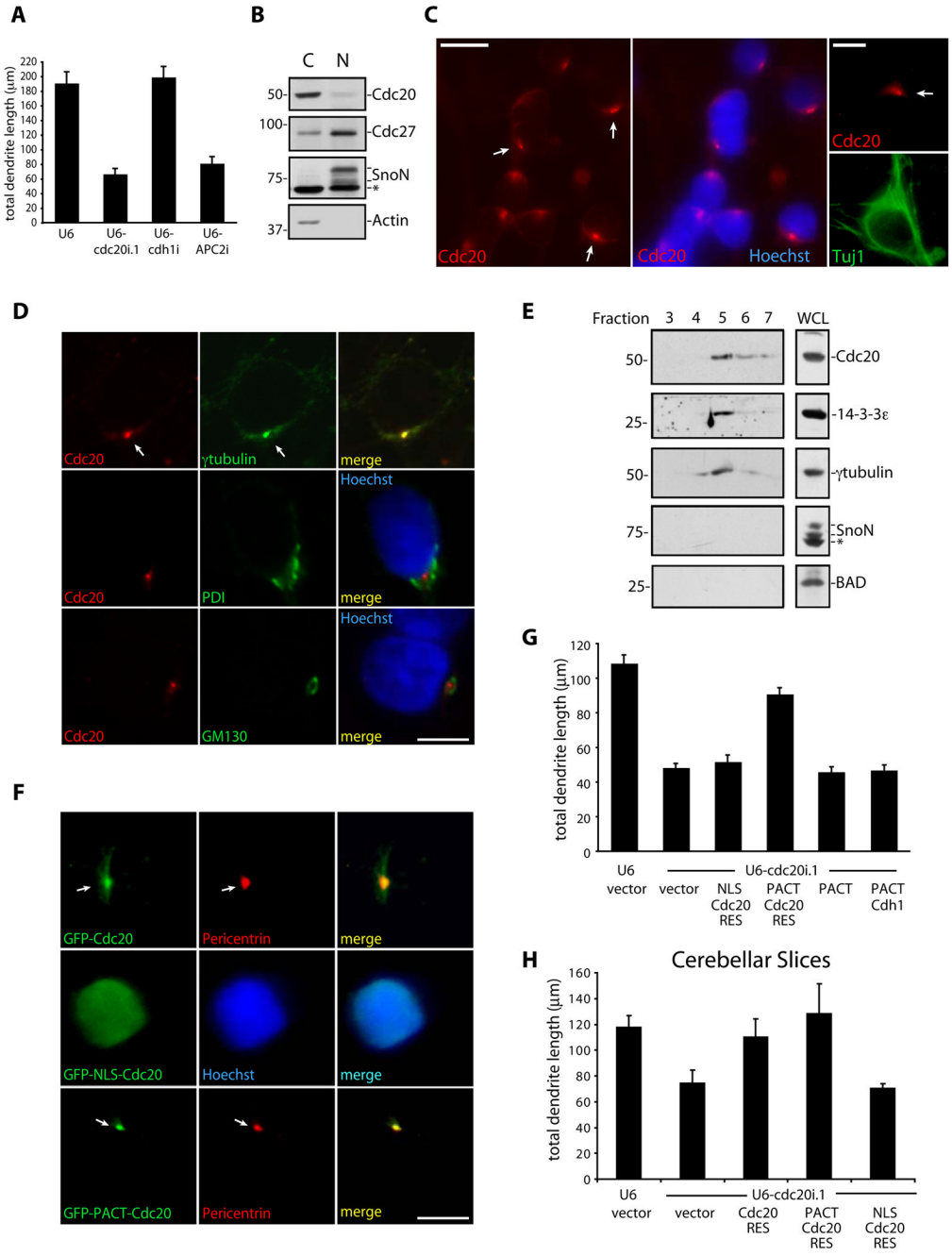

Figure 3. Cdc20-APC operates at the centrosome to promote dendrite development

(A) Granule neurons were transfected with the Cdc20, Cdh1, APC2, or control U6 RNAi plasmid together with a GFP expression plasmid and analyzed as in Figure 1C. Cdc20 or APC2 RNAi significantly decreased total dendrite length compared to control (ANOVA; $P < 0.0001$). 343 neurons were measured. APC2 RNAi also increased axon length in granule neurons (Figure S4B). **(B)** Granule neurons were subjected to subcellular fractionation and immunoblotted with the indicated antibodies. Actin and SnoN mark cytosolic (C) and nuclear (N) fractions, respectively. Asterisk indicates non-specific band. **(C)** Granule neurons were subjected to immunocytochemistry with the Cdc20 (red) and Tuj1 (green) antibodies as well as Hoechst nuclear staining (blue). Arrows indicate a perinuclear area of high Cdc20 immunoreactivity.

Cdc20 was observed in all cells labeled with the neuronal marker, Tuj1. Bar = 10 μm on the left and 5 μm on the right. **(D)** Granule neurons were subjected to immunocytochemistry using the Cdc20 antibody together with the γtubulin, protein disulphide isomerase (PDI), or GM130 antibody along with Hoechst nuclear labeling. Fluorescence was visualized by confocal microscopy. Arrows indicate the location of the centrosome, which is labeled with γtubulin. Bar = 5 μm. **(E)** Fractions isolated from a granule neuron centrosome preparation were immunoblotted using the indicated antibodies. Asterisk indicates non-specific band. WCL = whole cell lysate. **(F)** Granule neurons transfected with a GFP fusion expression plasmid encoding RNAi-resistant Cdc20, NLS-Cdc20, or PACT-Cdc20 were subjected to immunocytochemistry using the GFP antibody and, where indicated, the pericentrin antibody. Hoechst dye was used to label the nucleus. Arrows indicate co-localization of GFP-Cdc20 or GFP-PACT-Cdc20 with the centrosomal marker pericentrin. Bar = 5 μm. **(G)** Granule neurons were transfected with the Cdc20 RNAi or control U6 plasmid together with an expression plasmid encoding NLS-Cdc20-RES, PACT-Cdc20-RES, PACT, PACT-Cdh1, or control vector and a GFP expression plasmid and analyzed as in Figure 1C. PACT-Cdc20-RES, but not NLS-Cdc20-RES, PACT, or PACT-Cdh1, significantly increased total dendrite length compared to control vector in the background of Cdc20 knockdown (ANOVA, $P < 0.0001$). 789 neurons were measured. **(H)** Rat cerebellar slices transfected with the Cdc20 RNAi or control U6 plasmid together with the expression plasmid encoding Cdc20-RES, NLS-Cdc20-RES, PACT-Cdc20-RES, or control vector and a GFP expression plasmid were analyzed as in Figure 2A. Transfected IGL-resident neurons were quantified for total dendrite length. Cdc20-RES or PACT-Cdc20-RES but not NLS-Cdc20-RES significantly increased total dendrite length compared to control U6 transfection in the background of Cdc20 RNAi (ANOVA, $P < 0.0001$). 332 neurons were measured.

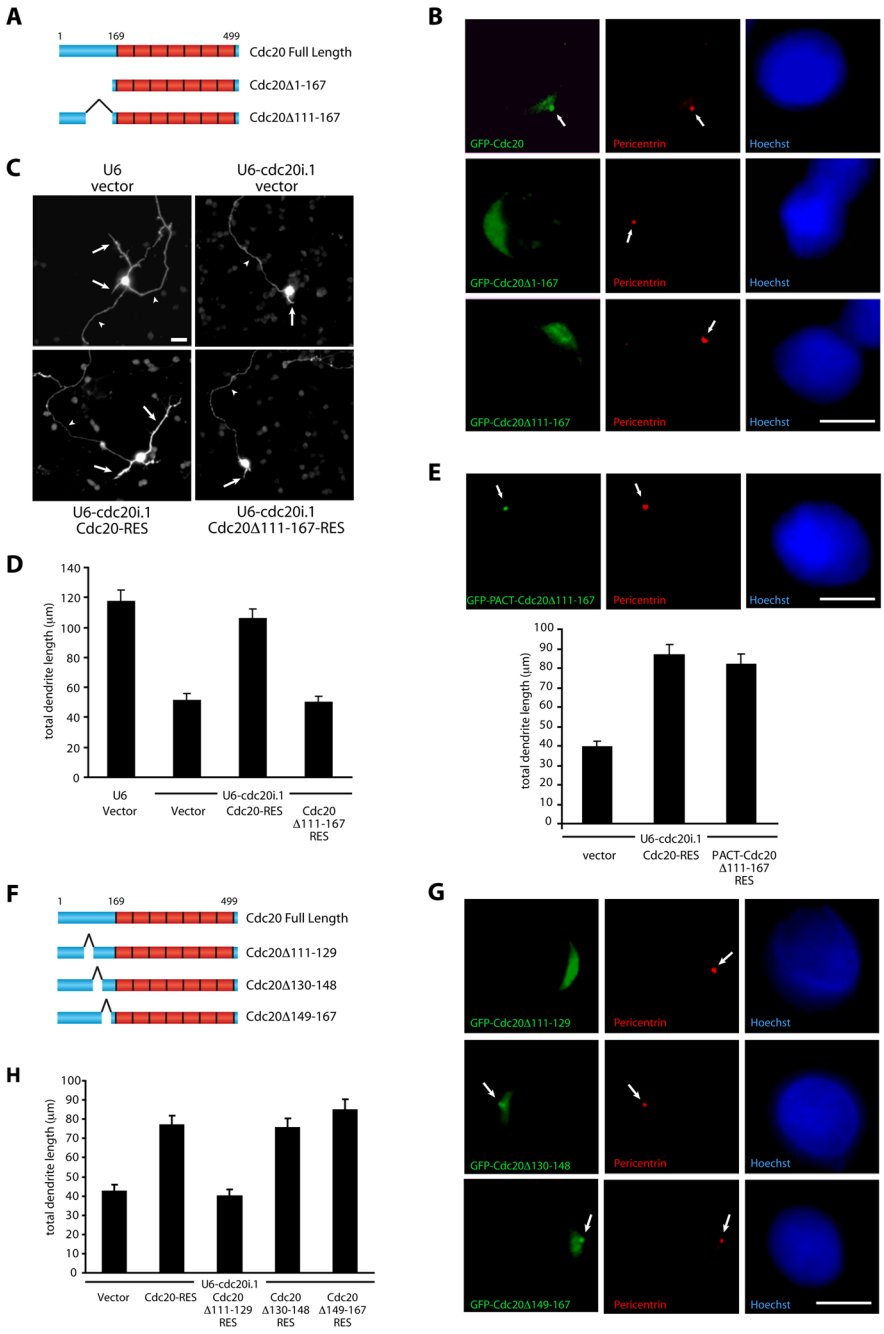

Figure 4. Identification of a centrosomal localization signal (CLS) that is required for Cdc20-dependent dendrite morphogenesis

(A) A diagram of Cdc20 deletion mutants evaluated for centrosomal localization. **(B)** Granule neurons transfected with a GFP fusion expression plasmid encoding RNAi-resistant Cdc20, Cdc20Δ1–167, or Cdc20Δ111–167 were subjected to immunocytochemistry using the GFP antibody and the pericentrin antibody to label centrosomes. Hoechst dye was used to label the nucleus. Arrows indicate co-localization of Cdc20 with pericentrin. Bar = 5 μm. **(C)** Granule neurons were transfected with the Cdc20 RNAi or control U6 plasmid together with the expression plasmid encoding Cdc20-RES, Cdc20Δ111-167-RES, or control vector and a GFP expression plasmid and analyzed as in Figure 1C. Bar = 10 μM. **(D)** Total dendrite length from

granule neurons treated as in (C) was quantified. Cdc20-RES, but not Cdc20Δ111-167-RES significantly increased total dendrite length compared to vector transfection in the background of Cdc20 knockdown (ANOVA, $P < 0.0001$). 360 neurons were measured. **(E)** Top: Granule neurons transfected with a GFP fusion expression plasmid encoding RNAi-resistant PACT-Cdc20Δ111–167 were analyzed as in (B). Arrows indicate co-localization of Cdc20 with pericentrin. Bar = 5 μm. Bottom: Granule neurons were transfected with the Cdc20 RNAi plasmid together with the expression plasmid encoding Cdc20-RES, PACT-Cdc20Δ111-167-RES, or control vector and a GFP expression plasmid. Neurons were analyzed as in Figure 1C. Cdc20-RES and PACT-Cdc20Δ111-167-RES significantly increased total dendrite length compared to vector transfection in the background of Cdc20 RNAi (ANOVA, $P < 0.0001$). 270 neurons were measured. **(F)** A diagram of Cdc20 mutants harboring deletions between amino acids 111–167. **(G)** Granule neurons transfected with a GFP fusion expression plasmid encoding RNAi-resistant Cdc20Δ111–129, Cdc20Δ130–148, and Cdc20Δ149–167 were analyzed as in (B). Arrows indicate co-localization of Cdc20 with pericentrin. Bar = 5 μm. **(H)** Granule neurons were transfected with the Cdc20 RNAi plasmid together with the expression plasmid encoding Cdc20-RES, Cdc20Δ111-129-RES, Cdc20Δ130-148-RES, Cdc20Δ149-167-RES, or control vector and a GFP expression plasmid and analyzed as in Figure 1C. Cdc20-RES, Cdc20Δ130-148-RES, and Cdc20Δ149-167-RES, but not Cdc20Δ111-129-RES, significantly increased total dendrite length compared to vector transfection in the background of Cdc20 RNAi (ANOVA, $P < 0.0001$). 300 neurons were measured.

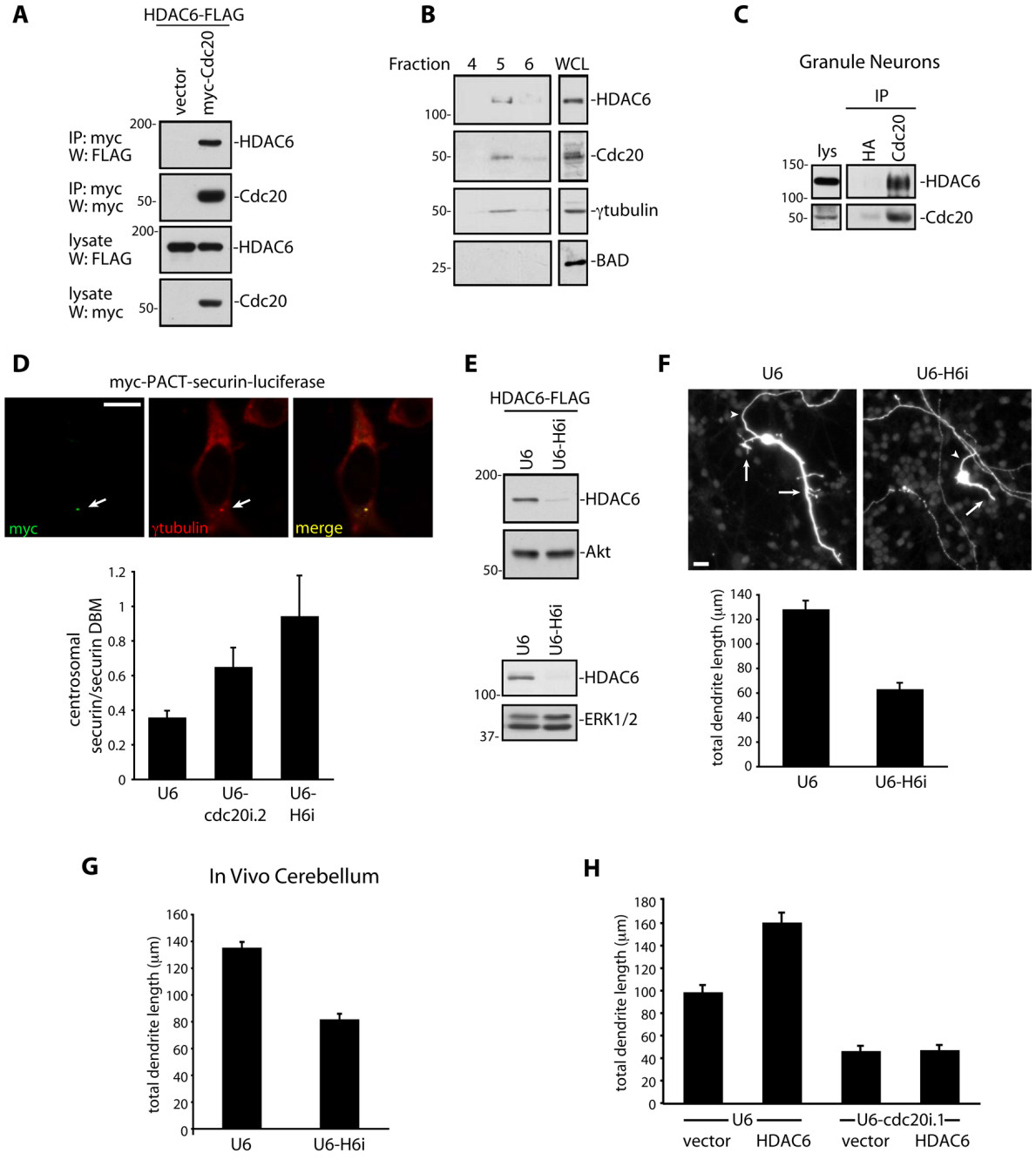

Figure 5. HDAC6 promotes Cdc20-APC function in neurons

(A) Lysates of 293T cells transfected with HDAC6-FLAG together with the myc-Cdc20 expression plasmid or control vector were immunoprecipitated using myc antibody, and immunoblotted with the indicated antibodies. **(B)** Granule neuron centrosome fractions prepared as in Figure 3E were immunoblotted with the indicated antibodies. **(C)** Granule neuron lysates were immunoprecipitated with the Cdc20 or control antibody (HA antibody) and immunoblotted with the indicated antibodies. **(D)** Top: 293T cells transfected with the myc-epitope-tagged PACT-securin-luciferase expression plasmid (myc-PACT-securin-luciferase) were subjected to immunocytochemistry with the myc and γtubulin antibodies. Arrows indicate co-localization of the securin-luciferase fusion protein with the centrosomal

marker γtubulin. Bar = 10 μM. Bottom: Granule neurons were transfected with the Cdc20 RNAi, HDAC6 RNAi, or control U6 plasmid together with the expression plasmid encoding myc-PACT-securin-luciferase or myc-PACT-securin-DBM-luciferase. Luciferase values obtained with securin-luciferase transfection were divided by those of securin DBM-luciferase (centrosomal securin/securin DBM) to generate a value inversely proportional to centrosomal Cdc20-APC activity. Knockdown of Cdc20 or HDAC6 in neurons significantly increased the relative amount of the centrosomal securin-luciferase reporter compared to control (Kruskal-Wallis; $P < 0.03$; n = 7). **(E)** Top: Lysates from COS cells transfected with HDAC6-FLAG together with the HDAC6 RNAi or control U6 plasmid were immunoblotted with the indicated antibodies. Bottom: Lysates from Neuro2A cells transfected with the HDAC6 RNAi or control U6 plasmid were immunoblotted with the indicated antibodies. **(F)** Granule neurons transfected with the HDAC6 RNAi or control U6 plasmid together with a GFP expression plasmid were analyzed as in Figure 1C. Representative neurons are shown (top), and total dendrite length is presented (bottom). Bar = 10 μm. HDAC6 knockdown significantly decreased total dendrite length compared to control (t-test; $P < 0.0001$). 186 neurons were measured. **(G)** Rat pups electroporated in vivo with U6-H6i/CMV-GFP RNAi or control U6/CMV-GFP plasmid were analyzed as in Figures 2C and 2D. HDAC6 RNAi significantly reduced granule neuron dendrite length compared to control (t-test; $P < 0.0001$). 132 neurons were measured. **(H)** Granule neurons transfected with the Cdc20 RNAi or control U6 plasmid together with the HDAC6 expression plasmid or control vector were analyzed as in Figure 1C. Expression of HDAC6 significantly increased total dendrite length compared to control. Expression of HDAC6 in the background of Cdc20 RNAi significantly reduced total dendrite length in neurons compared to transfection of the control U6 plasmid plus either the HDAC6 expression plasmid or vector (ANOVA; $P < 0.0001$). 371 neurons were measured.

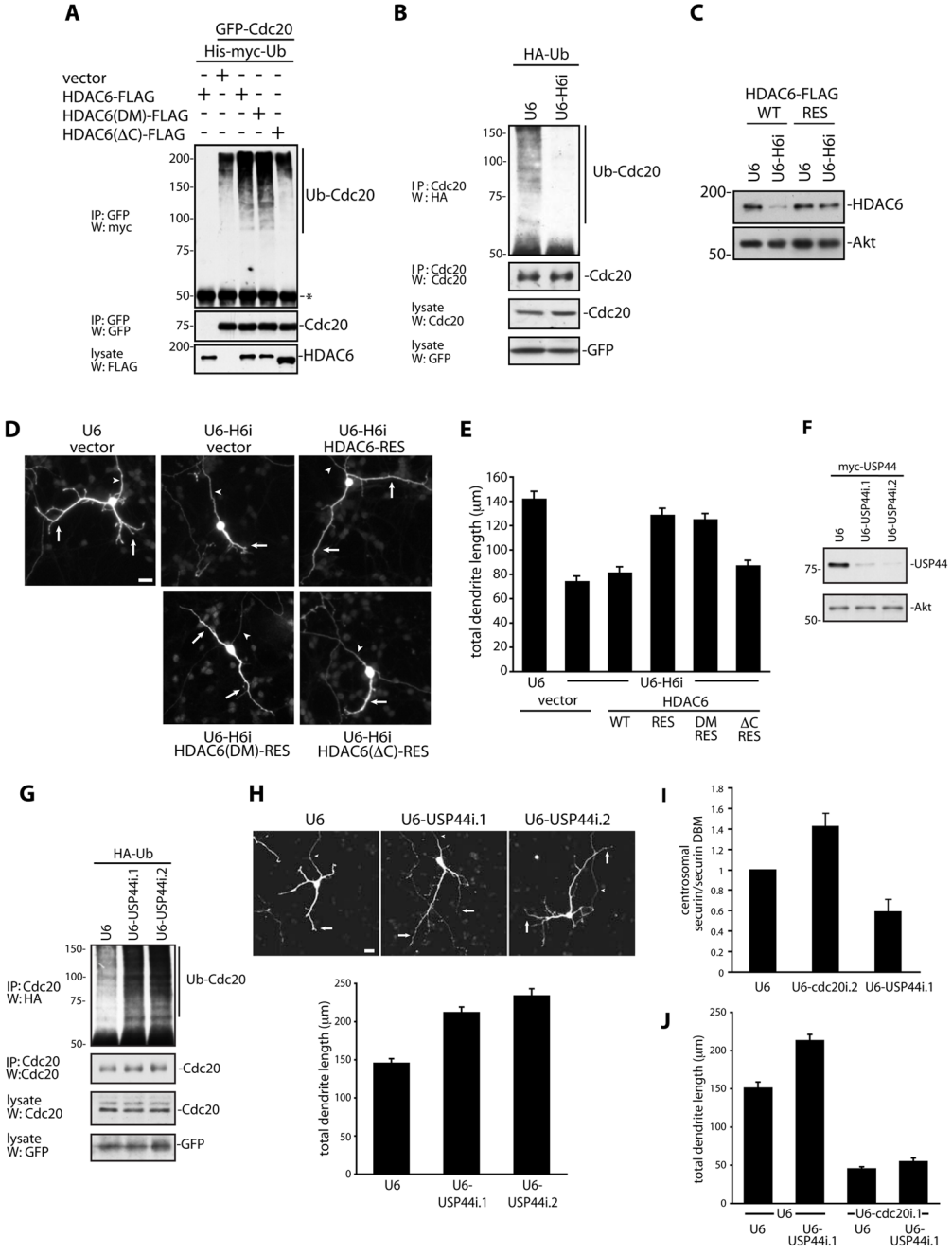

Figure 6. HDAC6 promotes Cdc20 polyubiquitination and dendrite morphogenesis

(A) Lysates of 293T cells transfected with the GFP-Cdc20 expression plasmid or control vector together with a His-myc-ubiquitin expression plasmid and the indicated FLAG-HDAC6 expression plasmids were sonicated and immunoprecipitated with the GFP antibody. Immunoprecipitates and lysates were immunoblotted with the indicated antibodies. Asterisk indicates IgG heavy chain. Quantification of Cdc20 polyubiquitination: Cdc20 alone 1.0; HDAC6+Cdc20 1.8; HDAC6(DM)+Cdc20 2.1; HDAC6(ΔC)+Cdc20 1.0. **(B)** Granule neurons were transfected with the HDAC6 RNAi or control U6 plasmid together with expression plasmids encoding HA-ubiquitin and GFP as a marker of transfection efficiency. Sonicated lysates were immunoprecipitated with the Cdc20 antibody. Immunoprecipitates and

lysates were immunoblotted with the indicated antibodies. **(C)** Lysates from COS cells transfected with FLAG-tagged HDAC6-WT or HDAC6-RES along with the HDAC6 RNAi or control U6 plasmid were immunoblotted with the indicated antibodies. **(D)** Granule neurons were transfected with the HDAC6 RNAi or control U6 plasmid together with an expression plasmid encoding HDAC6-RES, HDAC6(DM)-RES, HDAC6(ΔC)-RES, or control vector and a GFP expression plasmid and analyzed as in Figure 1C. Representative neurons are shown. Bar = 10 μm. **(E)** Total dendrite length of neurons treated as in (D) plus an additional transfection consisting of HDAC6 RNAi plus HDAC6-WT was quantified. HDAC6-RES or HDAC6(DM)-RES significantly increased total dendrite length as compared to control vector in the background of HDAC6 RNAi (ANOVA; $P < 0.0001$). 774 neurons were measured. **(F)** Lysates from COS cells transfected with the myc-USP44 expression plasmid together with one of two different USP44 RNAi plasmids or control U6 plasmid were immunoblotted with the indicated antibodies. **(G)** Granule neurons were transfected with a USP44 RNAi plasmid or control U6 plasmid together with expression plasmids encoding HA-Ub and GFP and analyzed as in (B). **(H)** Granule neurons transfected with a USP44 RNAi plasmid or control U6 plasmid together with a GFP expression plasmid were analyzed as in Figure 1C. Representative neurons are shown (top), and total dendrite length was quantified (bottom). Bar = 10 μm. USP44 knockdown significantly increased total dendrite length compared to control (ANOVA; $P < 0.0001$). 274 neurons were measured. **(I)** Granule neurons were transfected with the Cdc20 RNAi, USP44 RNAi, or control U6 plasmid together with myc-PACT-securin-luciferase or myc-PACT-securin-DBM-luciferase and analyzed as in Figure 5D. Luciferase values were normalized to those of control U6-transfected cells. USP44 knockdown significantly decreased and Cdc20 knockdown increased the amount of relative centrosomal securin-luciferase reporter compared to control. (Kruskal-Wallis; $P < 0.05$; n = 3). **(J)** Granule neurons transfected with the Cdc20 RNAi or control U6 plasmid together with the USP44 RNAi or control U6 plasmid were analyzed as in Figure 1C. USP44 knockdown significantly increased total dendrite length compared to control. Cdc20 RNAi in the background of USP44 RNAi significantly reduced total dendrite length compared to control U6 or USP44 RNAi plasmid plus U6 (ANOVA; $P < 0.0001$). 355 neurons were measured.

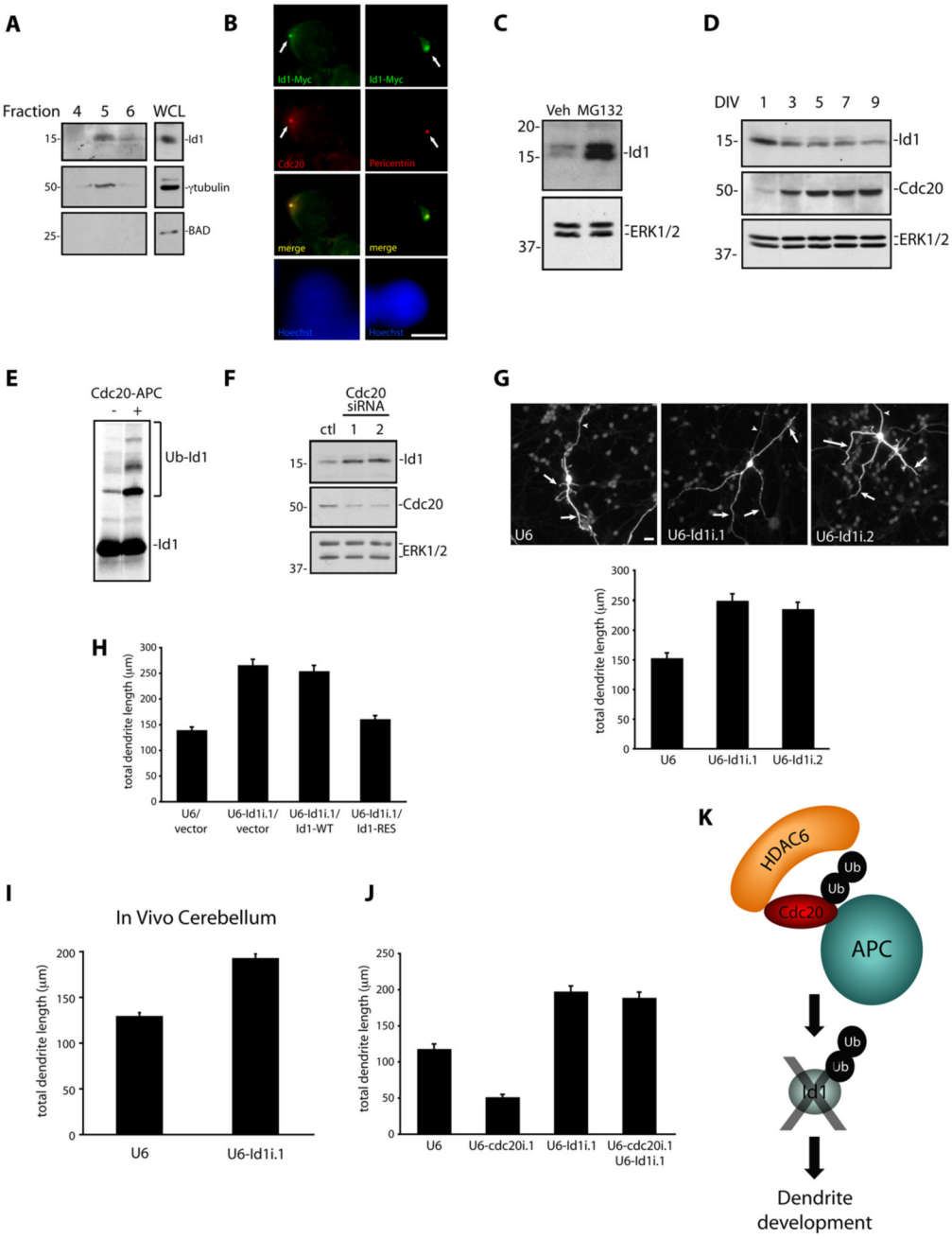

Figure 7. Cdc20-APC triggers the degradation of the centrosomal protein Id1

(A) Granule neuron centrosome fractions prepared as in Figure 3E were immunoblotted with the indicated antibodies. **(B)** Granule neurons transfected with the Id1-myc expression plasmid were subjected to immunocytochemistry with the myc antibody plus either the Cdc20 (left) or pericentrin (right) antibody. On the left, arrows indicate co-localization of Id1 with Cdc20. On the right, arrows indicate co-localization of Id1 with centrosomal marker pericentrin. Bar = 5 μm. **(C)** Lysates from granule neurons on DIV6 treated with MG132 (5 μM) or vehicle (DMSO) for 16 hr were immunoblotted with the indicated antibodies. **(D)** Lysates from granule neurons were immunoblotted with the indicated antibodies. DIV = days in vitro. **(E)** In vitro translated, ^{35}S-Met-labeled Id1 was incubated with or without immunopurified FLAG-Cdc20

and APC isolated from mitotic HeLa cells in an in vitro ubiquitination assay. Reaction products were resolved by SDS-PAGE followed by nitrocellulose transfer. Radioactivity was detected using PhosphorImager. **(F)** Lysates of granule neurons transfected with one of two distinct Cdc20 siRNAs for four days were immunoblotted with the indicated antibodies. ctl = scrambled sequence of Cdc20 siRNA.2. **(G)** Granule neurons transfected with an Id1 RNAi plasmid or control U6 plasmid together with a GFP expression plasmid were analyzed as in Figure 1C. Representative neurons are shown (top), and total dendrite length was quantified (bottom). Bar = 10 μm. Id1 knockdown using two distinct hairpins significantly increased total dendrite length compared to control U6 transfection (ANOVA; $P < 0.0001$). 294 neurons were measured. **(H)** Granule neurons were transfected with the Id1 RNAi or control U6 plasmid together with the expression plasmid encoding Id1-WT, Id1-RES, or control vector and the GFP expression plasmid and analyzed as in Figure 1C. Id1-RES but not Id1-WT decreased dendrite length in the background of Id1 RNAi (ANOVA; $P < 0.0001$). 352 neurons were measured. **(I)** Rat pups electroporated in vivo with the U6-Id1i.1/CMV-GFP RNAi or control U6/CMV-GFP plasmid were analyzed as in Figures 2C and 2D. Id1 RNAi plasmid significantly increased granule neuron dendrite length in vivo compared to control (t-test; $P < 0.0001$). 117 neurons were measured. **(J)** Granule neurons transfected with the Cdc20 RNAi or control U6 plasmid together with the Id1 RNAi or control U6 plasmid and GFP were analyzed as in Figure 1C. Cdc20 knockdown decreased total dendrite length compared to control. Id1 RNAi in the background of Cdc20 RNAi significantly increased total dendrite length in neurons compared to transfection of control U6 or Cdc20 RNAi plus U6 plasmids (ANOVA; $P < 0.0001$). 364 neurons were measured. (K) A model for the centrosomal HDAC6/Cdc20-APC/Id1 ubiquitin signaling pathway in postmitotic neurons.